Ion pair formation *via* photoinduced proton transfer in excited hydroxynaphthalimide-*N*-methylimidazole hydrogen bonded complex: effect of temperature and viscosity on dual fluorescence

László Biczók,[*a] Pierre Valat[b] and Véronique Wintgens[b]

[a] *Chemical Research Center, Hungarian Academy of Sciences, P.O. Box 17, 1525 Budapest, Hungary*
[b] *Laboratoire des Matériaux Moléculaires, C.N.R.S., E.R. 241, 2,8 rue H. Dunant, 94320 Thiais, France*

The kinetics of photoinduced processes in the hydrogen bonded complex between *N*-methyl-3-hydroxynaphthalimide and 1-methylimidazole was studied in a wide temperature range in ethyl acetate and glycerol triacetate. The proton transfer within the excited complex was found to be very fast because of its negligible activation energy. The fairly intense dual fluorescence was assigned to hydrogen bonded and solvent separated ion pairs. Kinetic parameters for the various deactivation pathways of these excited species were derived from the combined analysis of the steady-state and the time-resolved fluorescence results. The Arrhenius pre-exponential factor of the transition from the solvent separated into the hydrogen bonded ion pair proved to be more than two orders of magnitude larger in glycerol triacetate compared with that in ethyl acetate, whereas the other processes showed less viscosity dependence. The radiationless energy dissipation rate of the hydrogen bonded ion pair was insensitive to the experimental conditions. However, thermal enhanced internal conversion was observed for the solvent separated ion pair.

Introduction

It is well known that photoexcitation significantly enhances the acidity of hydroxyaromatic compounds.[1,2] The dynamics of the proton transfer from the excited molecule to solvent[3-6] or cluster of proton acceptors[7-9] have received widespread interest. However, much less attention has been devoted to the mechanistic details of the processes following the light absorption of hydrogen bonded complexes. Despite the fundamental importance of hydrogen bonding, for example in biological systems, molecular recognition and construction of large supramolecular architecture, it is not fully understood how the structure and the properties of the constituents and the media govern the various relaxation pathways of the excited hydrogen bonded complexes.

Different types of deactivation mechanisms were suggested for the excited complexes containing pyridine derivatives and aliphatic amines as the hydrogen bond acceptor component. Picosecond laser photolysis measurements on the complexes of 1-pyrenol with pyridine derivatives in hexane showed that the local excited state decays rapidly with time constant *ca.* 10 ps without producing any detectable long-lived intermediates.[10-12] Mataga *et al.* have concluded that coupled electron and proton displacement in the hydrogen bonded complex facilitates the charge transfer interaction between the two conjugate π-electronic systems and induces ultrafast excited state relaxation.[10-12] The fact that the fluorescence of 1-naphthol in the presence of pyridine is quenched completely even in a rigid glass[13] at 77 K is probably due to this type of deactivation process as well. In contrast, hydrogen bonded complexes of hydroxyarenes with aliphatic amines exhibit totally different behavior. Although they barely emit in fluid media around room temperature, fluorescence can be observed from the proton transferred species at low temperature.[14,15] It is well established that photoinduced proton

transfer from hydroxyarene to aliphatic amine is the primary process but the details of the subsequent reactions have not been clarified yet. The lack of systematic studies on the kinetics of the processes following the photoinduced proton transfer stems mainly from (i) the loss of fluorescence above *ca.* 200 K, (ii) the very similar characteristics and (iii) the large overlap among the spectra of contact, solvent separated and free ion pairs.[15]

We have recently shown that the hydrogen bonded complexes of hydroxynaphthalimides with imidazole and pyrazole exhibit unique behavior.[16] Their photoexcitation leads to fairly intense dual fluorescence in moderately polar solvents at room temperature. In the present studies, we exploit the special fluorescent characteristics of the hydrogen-bonded complex between *N*-methyl-3-hydroxynaphthalimide and 1-methyl-imidazole (Scheme 1) to examine the effect of temperature and viscosity on the dual fluorescence. To the best of our knowledge, this is the first time when the kinetics of processes following the photoinduced proton transfer within a hydrogen-bonded complex has been fully revealed in a wide temperature range.

The results on the photoinduced proton transfer and the subsequent ion pair separation in a phenol–imidazole type hydrogen bonded complex may contribute to the deeper understanding of the processes undergoing in proteins and peptides. Hydrogen bonded complexes of carboxylic acids

Scheme 1

DOI: 10.1039/b100692o

Phys. Chem. Chem. Phys., 2001, **3**, 1459–1464 **1459**
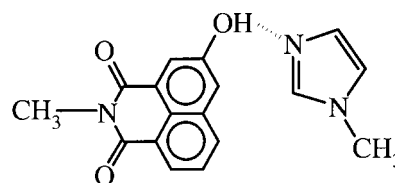
with 1-alkylimidazoles have received considerable attention[17–20] because they are excellent models of the active site of chymotrypsin. Hydrogen bonding between the phenol moiety of tyrosine and the imidazole group of histidine plays important role in the function of photosystem II in green plant photosynthesis.[21]

Experimental

3-Hydroxy-N-methyl-1,8-naphthalimide (3HONI), also called 5-hydroxy-2-methyl-1H-benz[d,e]iso-quinoline-1,3(2H)-dione, was synthesized as described previously.[16] N-Methylimidazole (Aldrich), ethyl acetate (Aldrich, spectroscopic grade) and glycerol triacetate (Prolabo) were used as received. The UV-visible absorption spectra were obtained with a Varian-Cary model 50 Bio apparatus. Fluorescence spectra were recorded with a SLM-Aminco model 8100 device. The temperature of the samples was controlled with an Oxford cryostat or a Lauda thermostatic bath. Fluorescence quantum yields were determined by comparison with that of 3-hydroxy-N-methyl-1,8-naphthalimide in CH_2Cl_2 solution, for which a reference yield of $\Phi_F = 0.13$ was taken.[16] Singlet lifetimes were measured by excitation with a B. M. Industries frequency-tripled Nd–YAG laser (pulse duration 30 ps FWHM), using the experimental set-up already described.[22]

Results and discussion

I. Steady-state measurements

Addition of N-methylimidazole (MIm) to a solution of 3HONI in ethyl acetate results in a characteristic change in the absorption spectrum (Fig. 1). The red shift of the long-wavelength band and the clear isosbestic points at 335.5, 345.5 and 384.5 nm indicate 1 : 1 hydrogen-bonded complex formation. From the absorbances measured in the absence and the presence of MIm (A_0 and A, respectively) at a particular wavelength (λ), the equilibrium constants of hydrogen bonding (K) can be determined using the following relationship:[23]

$$[1 - (A_0/A)_\lambda]/[\text{additive}] = -K + K(\varepsilon_C/\varepsilon_A)_\lambda(A_0/A)_\lambda \quad (1)$$

where $(\varepsilon_C/\varepsilon_A)_\lambda$ is the ratio of the molar absorption coefficients for the complexed and free 3HONI. The insert in Fig. 1 demonstrates that plotting the left-hand side of the function against $(A_0/A)_\lambda$ gives good linear correlation. From the intercepts 27 M^{-1} is obtained for the hydrogen bonding equilibrium constant. Similar behavior is found in a much more viscous and slightly more polar[24] solvent such as glycerol triacetate. In this solvent the average value of K calculated from the data measured at different wavelengths is 24 M^{-1}. The

fairly high values of the equilibrium constant ensure that the most of 3HONI is hydrogen bonded in the presence of 0.155 M MIm, and using 405 nm excitation light we can completely avoid emission originating from the uncomplexed 3HONI. In a previous paper[16] we have shown that the fluorescence maximum of 3HONI is at 411 nm. Since no emission can be detected below ca. 460 nm (Fig. 2), we can rule out interference from unbounded 3HONI.

We have recently found[16] that light absorption of the 3HONI–MIm hydrogen bonded complex (HB) leads to dual fluorescence in solvents of medium polarity. Fig. 2 presents representative spectra in ethyl acetate and glycerol triacetate. The large Stokes-shift indicates that the structure of the emitting species significantly differs from that of the ground state complex. It is well established that the charge density on the phenolic oxygen is reduced in the excited state and spread over the aromatic part of the molecule. This kind of electron displacement makes 3HONI much more acidic in the singlet excited state than in the ground state and causes a proton shift along the hydrogen bond in its MIm complex. Thus, the emission in the 480–600 nm spectral domain is assigned to excited hydrogen bonded ion pair (HBIP) which is formed in the ultrafast proton transfer from the HO-moiety of naphthalimide to the imidazole ring. The fluorescence band, which appears at higher wavelength, resembles that of the naphtholate anion of 3HONI, therefore, this band is attributed to solvent separated ion pair (SSIP). In this species the hydrogen bond is broken, each ion is fully solvated and Coulomb attraction ensures that the radical pair does not separate into the bulk of the nonpolar medium.

Fig. 2 demonstrates that the superimposition of the two bands can be resolved by assuming Gaussian shape for the spectral components. The results of the non-linear least-squares fit of the fluorescence spectra recorded at various temperatures in ethyl acetate and glycerol triacetate are summarized in Tables 1 and 2, respectively. The fluorescence maximum of the HBIP is scarcely sensitive to the temperature but cooling decreases the half-width of the peak. In contrast, significant blue shift and broadening is observed with decreasing temperature for the SSIP emission. These effects are attributed to the deceleration of the solvent relaxation at low
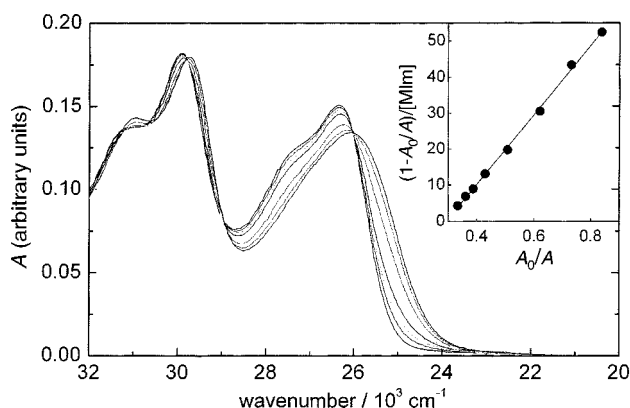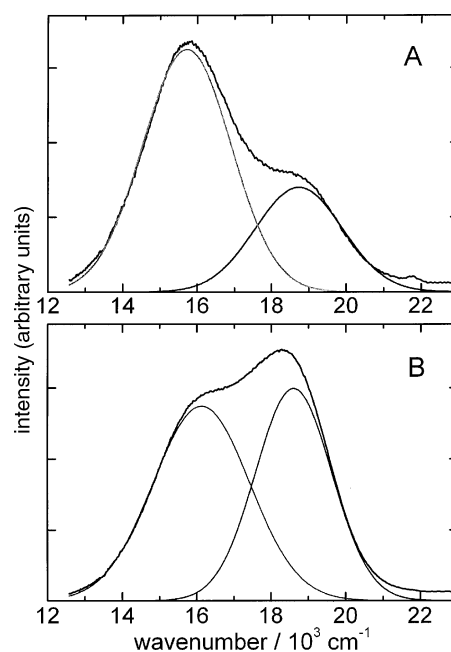

Fig. 1 Change of the 3HONI absorption spectrum on addition of MIm in ethyl acetate. Insert: determination of the hydrogen bonding equilibrium constant at 395 nm (see text).

Fig. 2 Dual fluorescence obtained by excitation of the 3HONI–MIm hydrogen bonded complex at 405 nm in ethyl acetate (A) and glycerol triacetate (B) at 293 K. The two bands are resolved by assuming a Gaussian shape for the spectral components.

Table 1 Temperature dependence of the dual emission of 3HONI–MIm complex in ethyl acetate, maxima ($\bar{v}_{max}$), half-widths (HW), fluorescence yields (Φ_F) and fluorescence decay parameters (λ)

T/K	Hydrogen bonded ion-pair				Solvent separated ion-pair			
	$\bar{v}_{max}$/cm^{-1}	HW/cm^{-1}	Φ_F(HBIP)	λ_1/10^8 s^{-1}	$\bar{v}_{max}$/cm^{-1}	HW/cm^{-1}	Φ_F(SSIP)	λ_2/10^8 s^{-1}
293	18 750	2140	0.0150	—[a]	15 540	1570	0.0411	4.35
288	18 720	2050	0.0150	—[a]	15 550	1590	0.0486	3.92
278	18 690	1900	0.0157	—[a]	15 610	1600	0.0614	3.25
269	18 710	1780	0.0163	—[a]	15 670	1630	0.0751	2.82
259	18 730	1650	0.0166	—[a]	15 720	1660	0.0936	2.37
249	18 730	1530	0.0176	21.7	15 760	1670	0.116	2.06
239	18 720	1430	0.0191	15.6	15 800	1680	0.142	1.58
230	18 710	1340	0.0216	10.6	15 830	1680	0.171	1.43
220	18 680	1290	0.0258	7.75	15 860	1690	0.206	1.17
215	18 650	1260	0.0304	6.33	15 890	1680	0.231	1.06
210	18 650	1230	0.0345	5.35	15 910	1700	0.254	0.935
205	18 630	1220	0.0407	4.27	15 930	1700	0.277	0.926
200	18 600	1210	0.0471	3.76	15 970	1710	0.297	0.813
195	18 580	1190	0.0587	2.86	16 020	1740	0.325	0.813
191	18 560	1180	0.0722	2.23	16 080	1760	0.351	0.710
185	18 550	1160	0.0882	1.73	16 200	1820	0.378	0.724
181	18 550	1140	0.106	1.23	16 370	1910	0.416	0.633
178	18 550	1100	0.112	1.01	16 550	2000	0.440	0.637

[a] Too large to be measured precisely.

temperature because more pronounced change occurs in glycerol triacetate whose viscosity shows larger temperature dependence. In addition to the spectral displacements, marked fluorescence intensity enhancement can be observed for both bands when the temperature is lowered (Fig. 3). The fluorescence yields given in Tables 1 and 2 clearly show monotone increase. However, the logarithm of the fluorescence yield ratio of the SSIP and the HBIP emissions (Φ(SSIP)/Φ(HBIP)) goes through a maximum in the function of the reciprocal temperature. The data given in Fig. 4 closely resemble the Steven–Ban plot that is derived for exciplex formation[25] suggesting that the transition between HBIP and SSIP in the excited state is a reversible process, as is shown in Scheme 2. k_S and k_R are the rate constants of the separation and the recombination of the hydrogen bonded ion pair, k_f and k'_f describe the rate constants of fluorescence emission, k_{nr} and k'_{nr} denote the non-radiative deactivation rate constants; unprimed and primed quantities refer to the hydrogen bonded (HBIP) and the solvent separated (SSIP) ion pairs, respectively. Based on the reaction scheme, the fluorescence yields are given by

$$\Phi(\text{HBIP}) = k_f(k'_f + k'_{nr} + k_R)/[(k_f + k_{nr})(k'_f + k'_{nr} + k_R) + k_S(k'_f + k'_{nr})] \quad (2)$$

$$\Phi(\text{SSIP}) = k'_f k_S/[(k_f + k_{nr})(k'_f + k'_{nr} + k_R) + k_S(k'_f + k'_{nr})] \quad (3)$$

$$\Phi(\text{SSIP})/\Phi(\text{HBIP}) = k'_f k_S/k_f(k'_f + k'_{nr} + k_R) \quad (4)$$

The radiative rate constants are usually considered temperature independent because the refractive index change with temperature causes much smaller effect than the temperature dependence of the nonradiative processes. Therefore, the increase of the fluorescence yield ratio with decreasing temperature is attributed to the deceleration of the ion pair recombination and/or the radiationless deactivation of the excited SSIP. At low temperature, the separation of the hydrogen bonded ion pair becomes dominant and the decline in Φ(SSIP)/Φ(HBIP) is due to the diminishing rate of this

Table 2 Temperature dependence of the dual emission of 3HONI–MIm complex in glycerol triacetate, maxima ($\bar{v}_{max}$), half-widths (HW), fluorescence yields (Φ_F) and fluorescence decay parameters (λ)

| T/K	Hydrogen bonded ion-pair				Solvent separated ion-pair			
	$\bar{v}_{max}$/cm^{-1}	HW/cm^{-1}	Φ_F(HB)	λ_1/10^8 s^{-1}	$\bar{v}_{max}$/cm^{-1}	HW/cm^{-1}	Φ_F(SS)	λ_2/10^8 s^{-1}
338	18 940	2710	0.0369	—[a]	15 500	1600	0.0587	2.87
329	18 810	2210	0.0308	—[a]	15 620	1590	0.0735	2.36
320	18 730	1990	0.0310	21.7	15 660	1610	0.0932	2.00
311	18 700	1790	0.0325	14.1	15 710	1650	0.120	1.68
302	18 640	1690	0.0384	10.0	15 740	1640	0.150	1.38
293	18 590	1590	0.0418	7.25	15 790	1650	0.169	1.20
284	18 580	1520	0.0550	4.76	15 830	1680	0.212	0.966
279	18 570	1500	0.0648	3.60	15 870	1700	0.234	0.872
274	18 570	1480	0.0767	3.11	15 920	1730	0.254	0.850
269	18 580	1460	0.0975	2.79	16 010	1780	0.278	0.847
264	18 600	1440	0.119	2.54	16 130	1840	0.298	0.757
260	18 630	1420	0.140	2.34	16 310	1920	0.316	0.671
255	18 680	1400	0.153	1.69	16 590	2050	0.333	0.606
250	18 750	1380	0.180	1.15	16 900	2100	0.342	0.499
245	18 820	1360	0.212	0.88	17 200	2200	0.342	0.457

[a] Too large to be measured precisely.
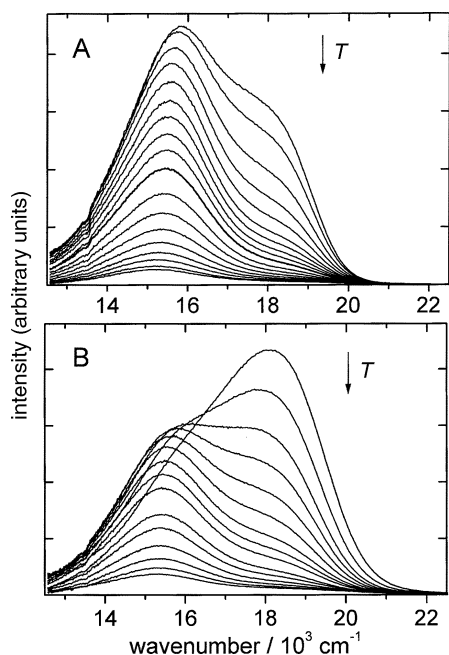
Fig. 3 Temperature dependence of the dual emission obtained by excitation of the 3HONI–MIm hydrogen bonded complex at 405 nm in ethyl acetate (A) and glycerol triacetate (B). The arrows show the direction of the temperature increase; temperatures are given in Tables 1 and 2.

process. Although the characteristic temperature dependence presented in Fig. 4 seems to be similar to the Steven–Ban plot of the exciplex to monomer fluorescence quantum yield ratio,[25] the usual kinetic treatment of this type of experimental data[26,27] can not be applied because not only the interconversion between HBIP and SSIP is temperature dependent but also the non-radiative deactivation of SSIP (*vide infra*).

II. Studies in glycerol triacetate glass at 77 K

The emission at long wavelength disappears in organic glass at 77 K and only one band is observed in the fluorescence spectrum (Fig. 5) which is attributed to the hydrogen bonded ion pair. The rigidity of the medium prevents the solvent separated ion pair formation. The large Stokes-shift indicates that photoinduced proton displacement along the hydrogen bond can take place readily even in low temperature rigid
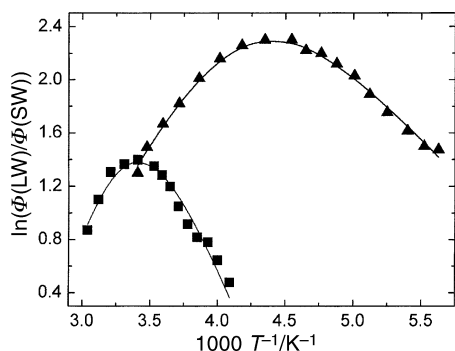

Fig. 4 Logarithm of the fluorescence yield ratio of the SSIP and the HBIP emissions in the function of the reciprocal temperature in ethyl acetate (▲) and glycerol triacetate (■). Line presents the fitted function.
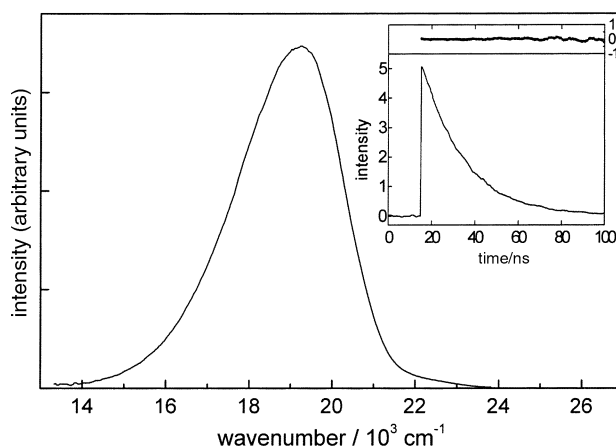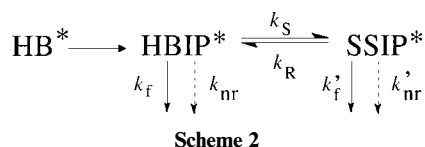

Scheme 2

Fig. 5 Fluorescence spectrum in glycerol triacetate glass at 77 K. Insert: fluorescence decay and the residual values of the single exponential fit.

glass. No well-defined fluorescence band is seen in the 420–470 nm spectral range, where the emission of the excited neutral hydrogen bonded complex (HB) could be expected. These observations further corroborate that the hydrogen bonded ion pair (HBIP) emits the intense fluorescence and the excited state proton transfer within the hydrogen-bonded complex is very fast because of its negligible activation energy.

The insert in Fig. 5 presents the fluorescence decay together with the residual values of the single exponential fit. The calculated reciprocal fluorescence lifetime is 5.0×10^7 s^{-1} that represents the sum of the fluorescence and radiationless deactivation rate constants of HBIP ($k_f + k_{nr}$). In contrast with the strong emission of triplet 3HONI[16] at 77 K, 3HONI + MIm complex does not phosphoresce. This suggests that internal conversion is the dominant process for the excited hydrogen bonded ion pair.

III. Time-resolved measurements

In order to gain deeper insight into the mechanism and the kinetics of the processes undergoing from the excited states, we carried out time-resolved fluorescence measurements. Fluorescence decays of HBIP and SSIP were monitored at 550 and 650 nm, respectively. The fluorescence intensity *vs.* time ($I(t)$) could be well described with double exponential function:

$$I(t) = C_1 \exp(-\lambda_1 t) + C_2 \exp(-\lambda_2 t) \qquad (5)$$

where λ_1, λ_2 are the decay parameters and C_1, C_2 denote the amplitudes. The short-lived decay component at 550 nm corresponded to the rise of the fluorescence recorded at 650 nm, whereas the long-lived components agreed at both wavelengths. The temperature dependence of the fitted λ_1, λ_2 values is given in Tables 1 and 2. The substantial overlap between the fluorescence of HBIP and SSIP prevented the derivation of kinetic information from the amplitude ratios (C_2/C_1). Based on Scheme 2, the decay parameters are defined by:

$$\lambda_{1,2} = 0.5\{(X + Y) \pm [(X - Y)^2 + 4k_S k_R)]^{1/2}\} \qquad (6)$$

where

$$X = (k_f + k_{nr} + k_S) \text{ and } Y = (k'_f + k'_{nr} + k_R).$$

The results presented in Fig. 4 suggest that the back formation of HBIP from SSIP in the excited state is fairly slow below 283 and 206 K in glycerol triacetate and ethyl acetate, respectively. Consequently, $4k_S k_R \ll (X - Y)^2$ in these temperature ranges and eqn. (6) can be reduced:

$$\lambda_1 = k_f + k_{nr} + k_S \qquad (7)$$

$$\lambda_2 = k'_f + k'_{nr} \qquad (8)$$

It is evident from the data shown in Tables 1 and 2 that both λ_1 and λ_2 decrease even at low temperature. The temperature dependence of the decay parameters can be well described by the following function:

$$\lambda = C + A \exp(-E/RT) \qquad (9)$$

Fitting eqn. (9) to the λ_2 experimental data below 206 and 283 K in glycerol triacetate and ethyl acetate, respectively, gives the activation energy $E = E'_{nr}$ and the preexponential factor $A = A'_{nr}$ for the radiationless deactivation of SSIP, whereas the C parameter represents its radiative rate constant ($C = k'_f$).

When eqn. (9) is fitted to the λ_1 values in the low temperature domain, C refers to the sum of the rate constants of the radiative and the non-radiative processes depopulating the excited HBIP ($C = k_f + k_{nr}$) and the Arrhenius parameters characterize the solvent separated ion pair formation. The $k_f + k_{nr}$ quantity does not show solvent dependence and agrees with the reciprocal fluorescence lifetime in glycerol triacetate at 77 K (*vide supra*). The calculated quantities are listed in Table 3.

IV. Kinetic and thermodynamic parameters

As the time-resolved studies indicate that not only the reversible transition between HBIP and SSIP is temperature dependent but also the nonradiative deactivation of SSIP, eqn. (4), leads to the following expression:

$$\frac{\Phi(\text{SSIP})}{\Phi(\text{HBIP})} = \frac{k'_f A_S \exp(-E_S/RT)}{k_f(k'_f + A_R \exp(-E_R/RT) + A'_{nr} \exp(-E'_{nr}/RT)}$$

$$(10)$$

If we use the kinetic parameters determined from the fluorescence decay measurements at low temperature, there are only three unknown quantities in this relation: the rate constant of HBIP fluorescence (k_f), and the Arrhenius factors (A_R, E_R) of the back formation of HBIP. These quantities were determined by fitting eqn. (10) to the temperature dependence of $\ln(\Phi(\text{SSIP})/\Phi(\text{HBIP}))$. It is apparent from Fig. 4 that the calculated functions describe well the experimental data. The derived kinetic parameters are summarized in Table 3 together with the enthalpy (ΔH) and entropy change (ΔS) in the reversible transition between HBIP and SSIP. The latter quantities were calculated using the following equations:

$$\Delta H = E_S - E_R \qquad (11)$$

$$\Delta S = R(\ln A_S - \ln A_R) \qquad (12)$$

When HBIP is transferred into SSIP, the solvation of the ions is increased with corresponding reduction of interionic Coulomb attractions. The considerable gain in enthalpy in the course of the solvation leads to negative ΔH. Despite the similar dielectric constants of ethyl acetate and glycerol triacetate, large difference was found between the ΔH values measured in these solvents indicating that the dielectric continuum model does not describe satisfactorily the solvation energy of the ion pairs. The strongly negative ΔS suggests that the entropy decrease connected with the solvate shell reorganization plays the dominant role.

The dynamics of excited state ion-pairing of 2-naphtholate salts have been studied in solvents of medium polarity and the exchange rate constants between excited contact and solvent separated ion pairs were found to be about 2×10^7 s^{-1} in tetrahydrofuran at room temperature.[28] Our results clearly demonstrate that these types of rate constants are strongly temperature and viscosity dependent. The relative magnitude of the Arrhenius parameters controls that the decrease of the thermal energy favors contact or solvent separated ion pair formation at a certain temperature. Cooling slows down the back formation of HBIP and hereby, stabilizes SSIP in the high temperature domain, whereas, it hinders the transition from HBIP to SSIP at low temperature.

It is especially noteworthy that among the kinetic parameters the A-factor of the SSIP → HBIP process exhibits the most substantial difference in the two solvents used in this study. The large A_R, found in glycerol triacetate reflects the complex nature of this quantity. As Saltier and D'Agostino suggested,[29] the Arrhenius parameters are composed of an inherent and a viscosity dependent component. Our A_R and E_R in glycerol triacetate are in accord with the corresponding values reported for photoisomerization in glycerol.[29] Taking the temperature dependence of viscosity from the literature,[30] we found the following correlations for glycerol triacetate and ethyl acetate, respectively:

$$(\eta/\text{cP})^{-1} = 8.40 \times 10^{13} \exp(-10120 \text{ K}/T)$$

$$= 8.40 \times 10^{13} \exp(-84.2 \text{ kJ mol}^{-1}/RT) \quad (13)$$

$$(\eta/\text{cP})^{-1} = 46.0 \exp(-892 \text{ K}/T)$$

$$= 46.0 \exp(-7.4 \text{ kJ mol}^{-1}/RT) \qquad (14)$$

These equations clearly demonstrate that the viscosity of ethyl acetate is much lower than that of glycerol triacetate and remains small over the entire temperature range. The activation energy of viscous flow in eqn. (14) ($E_\eta = 7.4$ kJ mol^{-1}) is significantly lower than E_S and E_R in ethyl acetate (Table 3). Therefore, viscosity does not play dominant role in determining the kinetics of the processes in this non-viscous solvent. On the contrary, the increase of the Arrhenius parameters in glycerol triacetate stems completely from the more restricted mobility within the solvate shell.

Many factors influence the kinetics of the interconversion between HBIP and SSIP. Coulombic interionic interactions must be considered in competition with ion–solvent dipole interactions. The transformation of SSIP into HBIP involves particularly substantial rearrangement of the solvent cage: (i) the solvent molecules escape from the space between the ions, and (ii) the decrease of the interion distance leads to cancellation of the orienting influence of the ions on the solvent shell. The solvent molecules are less ordered and weaker bounded around the HBIP compared to SSIP. Hence, the SSIP → HBIP process has large activation entropy, which explains the high frequency factor (A_R) of the reaction. The *ca.* two orders of magnitude smaller A-factor of the HBIP → SSIP reaction (A_S) in ethyl acetate arises from the lower activation entropy of this process. These facts seem to indicate that the structure of the transition state resembles more that of the HBIP. Also the relatively low E_S suggests that the hydrogen bond is not completely cleaved in the transition state because

Table 3 Kinetic and thermodynamic parameters

Solvent	$k_f/$ 10^7 s^{-1}	$k_{nr}/$ 10^7 s^{-1}	$A_S/$ 10^{13} s^{-1}	$E_S/$ kJ mol^{-1}	$A_R/$ 10^{15} s^{-1}	$E_R/$ kJ mol^{-1}	$k'_f/$ 10^7 s^{-1}	$A'_{nr}/$ 10^{10} s^{-1}	$E'_{nr}/$ kJ mol^{-1}	$-\Delta S/$ J K^{-1} mol^{-1}	$-\Delta H/$ kJ mol^{-1}
Glycerol triacetate	1.9	3.1	4.2	27.7	760	56.4	2.4	3.2	14.1	81	28.7
Ethyl acetate	1.9	3.1	2.6	14.6	4.7	29.0	2.4	1.1	4.3	43	14.4

the hydrogen bonding strength in the excited HBIP is expected to be higher than the activation energy of the solvent separated ion-pair formation in ethyl acetate ($E_S = 14.6$ kJ mol^{-1}). FTIR and NMR spectroscopic measurements showed[17–20] that strong, low-barrier hydrogen bond links MIm to a carboxylic acid of pK_a about 2.1. For example, 51.5 kJ mol^{-1} was reported[17] for the enthalpy of complex formation between MIm and dichloropropionic acid (p$K_a = 2.06$) in CHCl$_3$. As the pK_a^* of the singlet excited 3HONI is close to that of dichloropropionic acid,[31] the hydrogen bond is probably strong in the excited 3HONI–MIm hydrogen bonded ion pair as well.

In accordance with the expectations, the radiative and the internal conversion rate constants for HBIP are insensitive to the experimental conditions. Our results show that steady-state fluorescence measurements are not sufficient to reveal the mechanistic details of the deactivation kinetics. Time-resolved studies proved that the internal conversion of the excited solvent separated ion pair has temperature dependent rate. The effect is interpreted in terms of a thermal population of vibrationally active deactivating mode. As the excitation energy of SSIP is dissipated to the surrounding molecular bath, it is not surprising that the viscosity affects the activation energy of this process. The A'_{nr} factors obtained in this work are similar to the value reported for the temperature dependent internal conversion of 2-methoxyfluorenone in toluene (3.9×10^{10} s^{-1}).[32]

Acknowledgements

References

1 J. F. Ireland and P. A. H. Wyatt, *Adv. Phys. Org. Chem.*, 1976, **12**, 131.
2 P. Wan and D. Shukla, *Chem. Rev.*, 1993, **93**, 571.
3 K. M. Solntsev, D. Huppert, L. M. Tolbert and N. Agmon, *J. Am. Chem. Soc.*, 1998, **120**, 7981.
4 K. M. Solntsev, D. Huppert and N. Agmon, *J. Phys. Chem. A*, 1998, **102**, 9599.
5 L. M. Tolbert and J. E. Haubrich, *J. Am. Chem. Soc.*, 1994, **116**, 10593.
6 B. Cohen and D. Huppert, *J. Phys. Chem.*, A, 2000, **104**, 2663.
7 J. Lee, R. D. Griffin and G. W. Robinson, *J. Chem. Phys.*, 1985, **82**, 4920.
8 S. K. Kim, J. J. Breen, D. M. Willberg, L. W. Peng, A. Heikal, J. A. Syage and A. H. Zewail, *J. Phys. Chem.*, 1995, **99**, 7421.
9 M. Than Htun, A. Suwaiyan, A. Baig and U. K. A. Klein, *J. Phys. Chem.*, A, 1998, **102**, 8230.
10 H. Miyasaka, A. Tabata, S. Ojima, N. Ikeda and N. Mataga, *J. Phys. Chem.*, 1993, **97**, 8222.
11 H. Miyasaka, K. Wada, S. Ojima and N. Mataga, *Israel J. Chem.*, 1993, **33**, 183.
12 N. Mataga and H. Miyasaka, *Prog. React. Kinet.*, 1994, **19**, 317.
13 A. K. Mishra and H. Shizuka, *Chem. Phys. Lett.*, 1988, **151**, 379.
14 A. K. Mishra, M. Sato, H. Hiratsuka and H. Shizuka, *J. Chem. Soc., Faraday Trans.*, 1991, **87**, 1311.
15 A. K. Mishra and H. Shizuka, *J. Chem. Soc., Faraday Trans.*, 1996, **92**, 1481.
16 L. Biczók, P. Valat and V. Wintgens, *Phys. Chem. Chem. Phys.*, 1999, **1**, 4759.
17 L. A. Reinhardt, K. A. Sacksteder and W. W. Cleland, *J. Am. Chem. Soc.*, 1998, **120**, 13366.
18 C. S. Cassidy, L. A. Reinhardt, W. W. Cleland and P. A. Frey, *J. Chem. Soc., Perkin Trans. 2*, 1999, 635.
19 M. Garcia-Viloca, A. González-Lafont and J. M. Lluch, *J. Phys. Chem. A*, 1997, **101**, 3880.
20 J. B. Tobin, S. A. Whitt, C. S. Cassidy and P. A. Frey, *Biochemistry*, 1995, **34**, 6919.
21 J. A. Gerlt and P. G. Gassman, *J. Am. Chem. Soc.*, 1993, **115**, 11552.
22 P. Valat, V. Wintgens, J. Kossanyi, L. Biczók, A. Demeter and T. Bérces, *J. Am. Chem. Soc.*, 1992, **114**, 947.
23 N. Mataga and S. Tsuno, *Bull. Chem. Soc. Jpn.*, 1957, **30**, 368.
24 Relative permittivities are 6.03 for ethyl acetate at 298 K and 7.19 for glycerol triacetate at 293 K, *Landolt–Börnstein Zahlenwerte und Funktionen aus Physik, Chemie, Astronomie, Geophysik und Technik, Eigenschaften der Materie in ihren Aggregatzuständen, 6 Teil, Elektrische Eigenschaften I*, ed. K. H. Hellwege and A. M. Hellwege, Springer Verlag, Berlin–Göttingen–Heidelberg, 1959, pp. 635–643.
25 B. Stevens and M. I. Ban, *Trans. Faraday Soc.*, 1964, **60**, 1515.
26 J. B. Birks, *Organic Molecular Photophysics*, Wiley, London, 1975.
27 K. A. Zachariasse, *Trends Photochem. Photobiol.*, 1994, **3**, 211.
28 J. Ph. Soumillion, P. Vandereecken, M. Van Der Auweraer, F. C. De Schryver and A. Schanck, *J. Am. Chem. Soc.*, 1989, **111**, 2217.
29 J. Saltier and J. T. D'Agostino, *J. Am. Chem. Soc.*, 1972, **94**, 6445.
30 *Landolt–Börnstein Zahlenwerte und Funktionen aus Physik, Chemie, Astronomie, Geophysik und Technik, Eigenschaften der Materie in ihren Aggregatzuständen, 5a Teil, Transportphänomene I*, ed. L. Andrussow and B. Schramm, Springer Verlag, Berlin–Heidelberg–New York, 1969, pp. 216–706.
31 L. Biczók, P. Valat and V. Wintgens, unpublished results.
32 L. Biczók, T. Bérces and F. Márta, *J. Phys. Chem.*, 1993, **97**, 8895.